

Abstract

SnTe materials ($\text{Sn}_{1-x}\text{Pb}_x\text{Te}_{1-y}\text{Se}_y$) are one of the most flexible material platforms for exploring the interplay of topology and different types of symmetry breaking. We study symmetry-protected topological states in SnTe nanowires in the presence of various combinations of Zeeman field, s -wave superconductivity and inversion-symmetry-breaking field. We uncover the origin of robust corner states and hinge states in the normal state. In the presence of superconductivity, we find inversion-symmetry-protected gapless bulk Majorana modes, which give rise to quantized thermal conductance in ballistic wires. By introducing an inversion-symmetry-breaking field, the bulk Majorana modes become gapped and topologically protected localized Majorana zero modes appear at the ends of the wire.

Topological states in the presence of Zeeman field

Our starting is the p -orbital tight-binding Hamiltonian which has been used for describing the bulk topological crystalline insulator phase in the SnTe materials [2] and various topological phases in lower dimensional systems [4, 1]

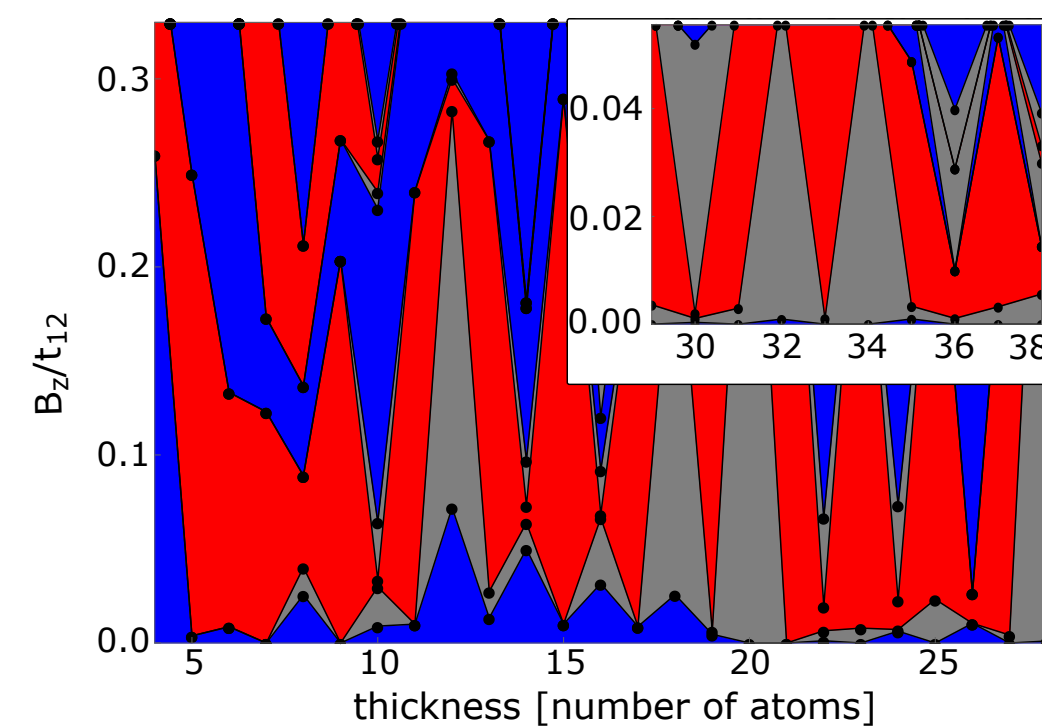


Figure 1:Phase diagram as function of the nanowire thickness (dimensions of the square cross-section) and Zeeman field B_z . The different phases are: insulator phase (blue), Weyl semimetal phase (red) and indirect semimetal phase (grey). In the regime of large Zeeman field the insulator phase supports a pseudospin texture due to band inversion, resulting in the appearance of localized corner states (see Fig. 2). Dots show the actually computed phase boundaries at discrete values of the wire thickness.

We study the properties of the system in the presence of Zeeman field $\mathcal{H}_Z = \mathbf{B} \cdot \vec{\sigma}$ applied along the wire $\mathbf{B} = (0, 0, B_z)$.

Hinge states

We find that the hinge states appear in the absence of Zeeman field and they resemble the protected states appearing in higher-order topological phases [3, 5]

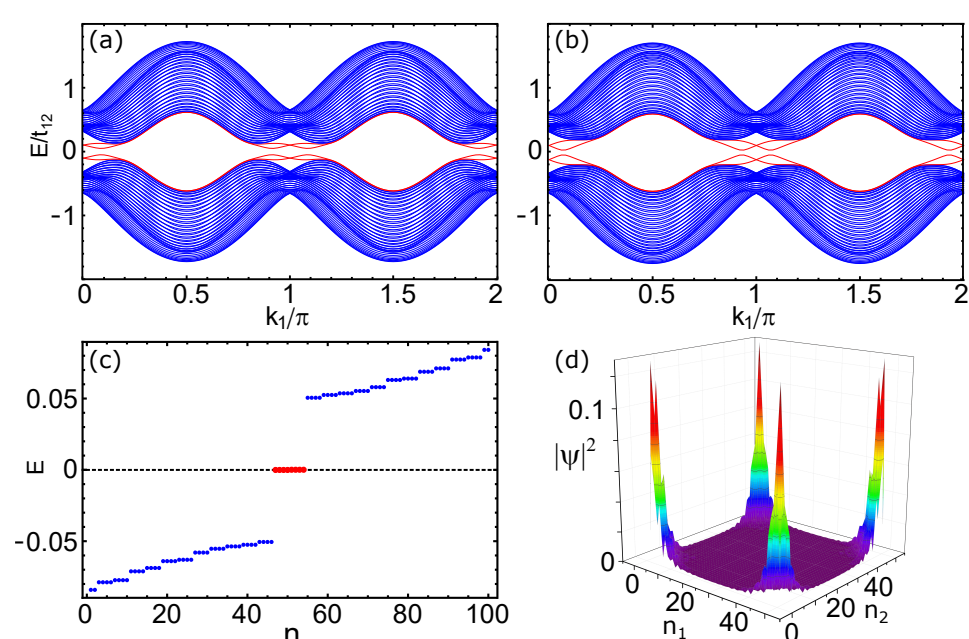


Figure 2:(a) Low-energy spectrum of the Hamiltonian $\mathcal{H}(k_1, k_2, k_3 = \pi)$ for $\lambda_z = 0$ in the case of open boundary conditions in the a_2 direction. The width of the system is 50 unit cells. (b) The low-energy spectrum in the case of uniform spin-orbit coupling $\lambda_\alpha = \lambda$ ($\alpha = x, y, z$). (c) Spectrum for $\lambda_z = 0$ in the case of open boundary conditions in both a_1 and a_2 directions. The red dots show the 8 zero-energy corner states. The system size is 50×50 unit cells. (d) LDOS of the corner states. Here, n_1 and n_2 label the unit cells in the directions of a_1 and a_2 , respectively.

The \mathbb{Z}_2 invariant ν can be determined using d and p as

$$\nu = (1 - \text{sgn}(pd))/2. \quad (1)$$

with $d = m((m - 2t_{11})^2 + 4t_{12}^2) - 2(m - 2t_{11})\lambda^2$ and $p = (m - 4t_{11})(m + 2t_{11})^2 - 2m\lambda^2$.

The topological phase diagram in the m - λ plane

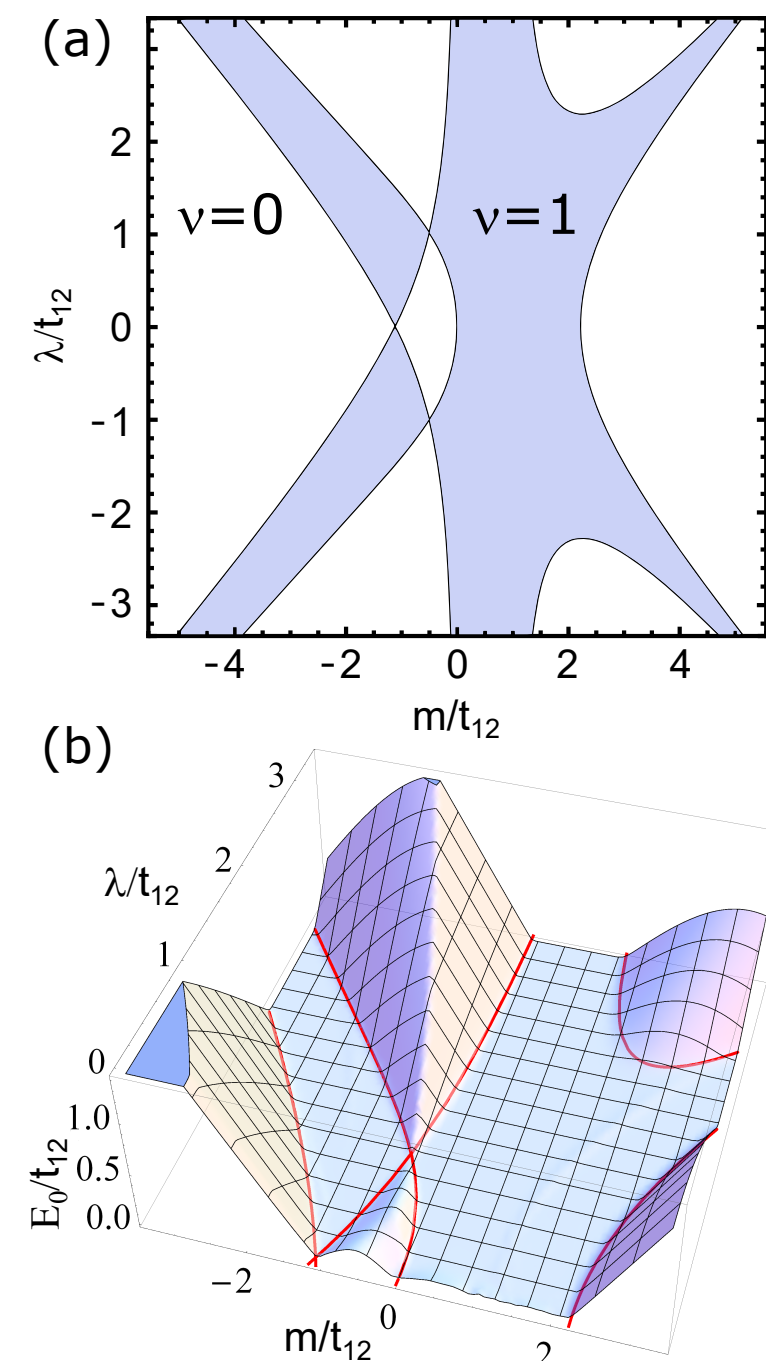


Figure 3:(a) Topological invariant ν [Eq. (1)] of the 2D Hamiltonian $\mathcal{H}(k_1, k_2, \pi)$ in the chiral limit $\lambda_z = 0$ and $\lambda_x = \lambda_y = \lambda$ as function of m and λ . The shaded region is the non-trivial phase $\nu = 1$ supporting corner states. (b) Energy of a state being closest to the zero energy in the system with all edges open, as function of m and λ . The red lines are phase boundaries from (a). The system size is 50×50 unit cells

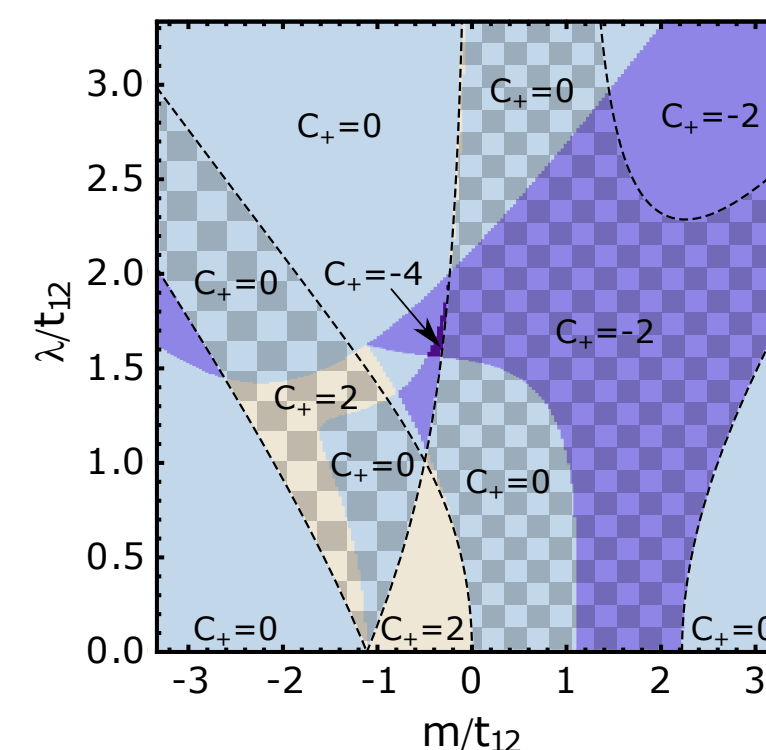


Figure 4:Topological phase diagram of Hamiltonian $\mathcal{H}(k_1, k_2, k_3)$ in the m - λ plane. Colors indicate different mirror M_{xy} Chern numbers C_+ defined in the k_1 - k_3 plane (with $k_2 = k_1$). Areas bounded by the dashed line and filled with checkerboard pattern are non-trivial in the sense of ν invariant of Eq. (1), also shown in Fig. 3. The chiral limit is assumed with $\lambda_z = 0$ and $\lambda_x = \lambda_y = \lambda$.

Majorana modes in the presence of superconductivity

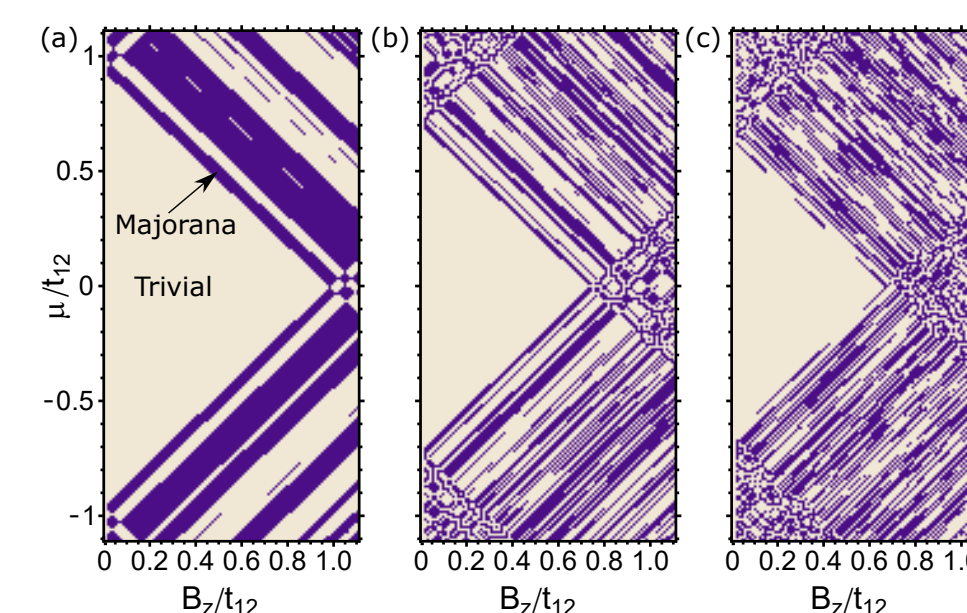


Figure 5:Topological phase diagrams for SnTe nanowires in presence of induced superconductivity. The thicknesses of the nanowires are (a) 8, (b) 10 and (c) 18 atoms. The blue regions indicate parameter regimes where $\nu_{sc} = 1$. In the presence of inversion symmetry they correspond to a topological phase supporting gapless Majorana bulk modes. If the inversion symmetry is broken they correspond to fully gapped topological superconducting phase supporting Majorana end modes. In the numerical calculations we have used $\Delta = 0.01$ eV. The topological region always starts for $B_z > \Delta$ and the main effect of increasing (decreasing) Δ is to shift the nontrivial phases right (left) along B_z axis.

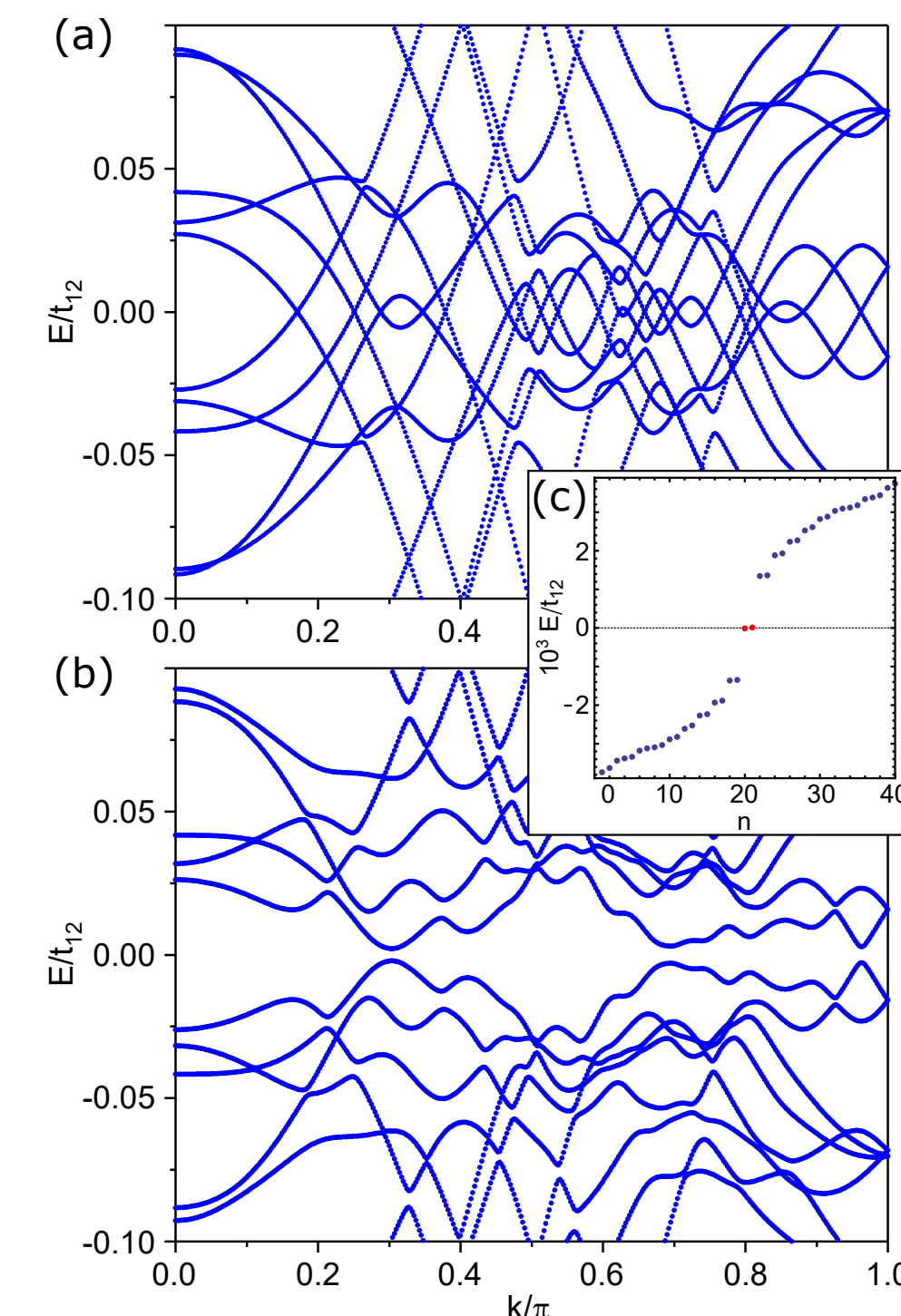


Figure 6:Band structures for 8 atoms thick superconducting nanowires (a) in the presence of inversion symmetry $\lambda_R = 0$ and (b) in the absence of inversion symmetry $\lambda_R = 0.05$ eV. (c) The spectrum for 400 atoms long superconducting nanowire in the absence of inversion symmetry $\lambda_R = 0.05$ eV demonstrating the existence of zero-energy Majorana modes localized at the end of the wire (red dots). For illustration purposes, we have computed the spectra for very thin nanowires with $B_z = 0.16$ eV, $\mu = 0.91$ eV and $\Delta = 0.1$ eV. However, due to the general arguments presented in the text, qualitatively similar results are expected also for experimentally feasible values of B_z , μ and Δ in thicker nanowires.

Discussion and conclusions

1. We have shown that SnTe materials support robust corner states and hinge states, which can be understood by \mathbb{Z}_2 invariant.
2. From the general trends in the thickness dependence we can extrapolate that for realistic nanowire thicknesses the topologically nontrivial phases can be reached with experimentally feasible values of the Zeeman field.
3. The superconducting SnTe nanowires support gapless bulk Majorana modes in the presence of inversion symmetry, and by introducing inversion-symmetry-breaking field, the bulk Majorana modes become gapped and topologically protected localized Majorana zero modes appear at the ends of the wire.

Acknowledgements

The work is supported by the Foundation for Polish Science through the IRA Programme co-financed by EU within SG OP. W.B. also acknowledges support by Narodowe Centrum Nauki (NCN, National Science Centre, Poland) Project No. 2019/34/E/ST3/00404.

References

- [1] W. Brzezicki, M. M. Wysockiński, and T. Hyart. Topological properties of multilayers and surface steps in the SnTe material class. *Phys. Rev. B*, 100:121107, Sep 2019.
- [2] T. H. Hsieh, H. Lin, J. Liu, W. Duan, A. Bansil, and L. Fu. Topological crystalline insulators in the SnTe material class. *Nature Communications*, 3:982, 2012.
- [3] F. Schindler, A. M. Cook, M. G. Vergniory, Z. Wang, S. S. P. Parkin, B. A. Bernevig, and T. Neupert. Higher-order topological insulators. *Science Advances*, 4(6):eaat0346, 2018.
- [4] P. Sessi, D. Di Sante, A. Szczepakow, F. Glott, S. Wilfert, H. Schmidt, T. Bathon, P. Dziawa, M. Greiter, T. Neupert, G. Sangiovanni, T. Story, R. Thomale, and M. Bode. Robust spin-polarized midgap states at step edges of topological crystalline insulators. *Science*, 354(6317):1269–1273, 2016.
- [5] L. Trifunovic and P. W. Brouwer. Higher-Order Bulk-Boundary Correspondence for Topological Crystalline Phases. *Phys. Rev. X*, 9:011012, Jan 2019.

Contact

Minh.Nguyen.Nguyen@MagTop.ifpan.edu.pl
brzezicki@magtop.ifpan.edu.pl
hyart@magtop.ifpan.edu.pl

For simplicity we consider a Rashba coupling term: $H_R(\mathbf{k}) = \lambda_R(\sin k_z \sigma_x - \sin k_x \sigma_z)$